ORIGINAL ARTICLE / ÖZGÜN MAKALE

PACLITAXEL-LOADED POLYCAPROLACTONE NANOPARTICLES FOR LUNG TUMORS; FORMULATION, COMPREHENSIVE *IN VITRO* CHARACTERIZATION AND RELEASE KINETIC STUDIES

AKCİĞER TÜMÖRLERİNE YÖNELİK PAKLİTAKSEL YÜKLÜ POLİKAPROLAKTON NANOPARTİKÜLLERİ; FORMÜLASYON, KAPSAMLI İN VİTRO KARAKTERİZASYON VE SALIM KİNETİK ÇALIŞMALARI

Sedat ÜNAL[1] ⓘ **, Osman DOĞAN[2]** ⓘ **, Yeşim AKTAŞ[1]*** ⓘ

[1]Erciyes University, Faculty of Pharmacy, Department of Pharmaceutical Technology, 38280, Kayseri, Turkey

[2]Abdullah Gül University, Faculty of Life and Natural Sciences, Bioengineering Department, 38080, Kayseri, Turkey

ABSTRACT

Objective: *Today, cancer is still among the most common chronic diseases. Nanoparticular drug delivery systems prepared with biocompatible and biodegradable polymers such as polycaprolactone are rational solution for anticancer agents with poor solubility and low bioavailability. The aim of this study is to prepare paclitaxel-loaded polycaprolactone nanoparticles, which is known to be a potent anticancer, and to elucidate in vitro characteristics and release kinetic mechanisms.*

Material and Method: *It was aimed to prepare paclitaxel-loaded polycaprolactone nanoparticles by nanoprecipitation. Preformulation studies were carried out with different molecular weights of polycaprolactone (Mw: 14.000, Mw: 80.000). Nanoparticles were coated with Chitosan or Poly-l-lysine to obtain cationic surface charge and to increase cellular interaction. Comprehensive characterization of formulations and release kinetic studies were performed.*

Result and Discussion: *The particle size of the formulations ranged from 188 nm to 383 nm. Encapsulation efficiency increased to 77% in different formulations. SEM analysis confirmed the nanoparticles were spherical. Within the scope of in vitro release studies, the release continued for up to 96 hours and less than 50% of the therapeutic load was released in the first 24 hours. Mathematical modeling indicated that the*

---
* **Corresponding Author / Sorumlu Yazar:** Yeşim Aktaş
e-mail / e-posta: yaktas@erciyes.edu.tr, **Phone / Tel.:** +905057154102

release kinetics fit more than one model with the Korsmeyer-Peppas, Peppas-Sahlin and Weibull models, which show high correlation.

Keywords: *Chitosan, lung cancer, paclitaxel, polikaprolakton, poly-l-lysine*

ÖZ

Amaç: *Günümüzde kanser hala en sık görülen kronik hastalıklar arasında yer almaktadır. Polikaprolakton gibi biyouyumlu ve biyoparçalanır polimerlerle hazırlanan nanopartiküler ilaç taşıyıcı sistemler, düşük çözünürlük ve düşük biyoyararlanım gösteren birçok antikanser ajan için rasyonel bir çözümdür. Bu çalışmanın amacı, güçlü bir antikanser olduğu bilinen paklitaksel yüklü polikaprolakton nanopartiküllerinin hazırlanması ve hazırlanan nanopartiküllerin in vitro karakterizasyonlarını ve salım kinetik mekanizmalarını aydınlatmaktır.*

Gereç ve Yöntem: *Nanoçöktürme yöntemi ile paklitaksel yüklü polikaprolakton nanopartiküllerinin hazırlanması amaçlanmıştır. Polikaprolakton polimerinin iki farklı moleküler ağırlığı (Mw: 14.000 ve Mw: 80.000) ile ön formülasyon çalışmaları yapılmıştır. Hazırlanan nanopartiküller, katyonik yüzey yükü elde etmek ve hücresel etkileşimi artırmak için Chitosan (CS) veya Poly-l-lisin (PLL) ile ayrı ayrı kaplanmıştır. Formülasyonların kapsamlı karakterizasyon çalışmaları ve salım kinetik çalışmaları yapılmıştır.*

Sonuç ve Tartışma: *Formülasyonların partikül boyutu 188 nm ila 383 nm arasında değişmektedir. Enkapsülasyon etkinliği, farklı formülasyonlarda %77'ye kadar yükselmiştir. SEM analizi, nanopartiküllerin küre şeklinde olduğunu doğrulamıştır. İn vitro salım çalışmaları kapsamında 96 saate kadar salım devam etmiş ve ilk 24 saatte terapötik yükün %50'sinden azı salınmıştır. Matematiksel modelleme çalışmaları, formülasyonların salım kinetiğinin, yüksek korelasyon gösteren Korsmeyer-Peppas, Peppas-Sahlin ve Weibull modelleri ile birden fazla modele uyduğunu göstermiştir.*

Anahtar Kelimeler: *Akciğer kanseri, kitosan, paklitaksel, polikaprolakton, poli-l-lizin*

INTRODUCTION

Cancer is a leading cause of death throughout the world, characterized by metastasis and uncontrolled proliferation. Approximately, 40% of cancer cases consists of breast, lung, prostate, stomach, colon, and skin cancer [1]. Among them, lung cancer is one of the most commonly diagnosed cancers in both men and women. Lung cancer related deaths account for approximately 20% of total cancer related deaths [2]. Lung cancer is classified into two main types, non-small cell lung cancer (NSCLC) and small cell lung cancer (SCLC). NSCL accounting for %87 of total lung cancer cases, is highly resistant to treatment including surgery, radiotherapy and chemotherapy [3]. Despite recent advances in cancer treatment, patients with lung cancer still have few therapeutic options and a very low survival rate which remains under 20%, due to poor prognosis, late diagnosis, development of drug resistance as well as low tumor selectivity [4]. In addition to these shortages, current traditional chemotherapeutics not only have limited efficacy but also cause systemic adverse effects which are among the most important factors in treatment discontinuation [5]. Another disadvantage of current traditional chemotherapeutic agents is that extremely high dose needs to be used in order to provide effective treatment. Thus, healthy tissue cells die more, and it is more likely to occur multi-drug resistance [6]. Given all of these drawbacks, it is obvious that a novel effective treatment method is required to increase the survival rate of lung cancer.

Paclitaxel (PCX) is a natural product isolated from North American Pacific yew tree, Taxus

brevifolia. Shortly after the discovery of PCX, it was found that PCX exhibited high anti-cancer activity [7]. Today PCX is one of the widely utilized molecules for an effective treatment of cancers namely lung, ovarian, breast and other cancer types. PCX is a classical microtubule inhibitor that acts by inhibiting the depolymerization of microtubules and block cancer cell at the G2/M phase [8]. Although PCX seems to be an acceptable candidate as anti-cancer agent, its severe side effects restrict the use of PCX in cancer therapy. PCX also adversely influences healthy cell such as immune system cells which may result in escaping tumor cells and the propagation of drug-resistant clones [9]. Another issue that relates to the drawback of PCX is the poor solubility of PCX in water (less than 1 µg/ml) [10]. Owing to its poor aqueous solubility, natural form of PCX cannot be used efficiently in treatment.

Nanomedicine provides a wide range of benefits that can overcome significant obstacles which other conventional chemotherapeutics suffer from and increase the survival rate in cancer treatment. Therefore, in recent years, enormous time and effort have been dedicated to developing nanotechnological approaches. Nanotechnology-based drug delivery systems offer longer circulation time, accumulation in targeted area, controlled release profile, resulting in more efficient therapeutic effect [11]. In particular many anti-cancer agents currently used in treatment such as paclitaxel, docetaxel, camptothecin have quite poor aqueous solubility due to their large polycyclic nature [12]. Nanoparticles (NPs) may also help to solve solubility problem of hydrophobic molecules [13]. After it has been realized that NPs is a promising carrier to encapsulate and deliver poorly soluble molecules, different types of NPs have been developed including carbon-based nanoparticles, metal nanoparticles, polymeric nanoparticles, lipid-based nanoparticles. Among them, polymeric NPs have emerged as promising carrier platform because of their capability of high drug entrapment, biocompatible properties and protection against drug degradation [14]. Polycaprolactone (PCL) is a semi-crystalline aliphatic polyester approved by FDA (Food and Drug Administration) to be used in clinical studies. High drug permeability, slow in vivo degradation as well as non-toxic properties of PCL make it a suitable polymer for drug delivery. In order to achieve an outstanding therapeutic potential, PCL has been combined with various drugs such as docetaxel, campthotecin, mitomycin C [15-17]. Various modifications can be made with a state-of-art approach in the design of PCL-based nanoparticulate drug delivery systems in order to increase the therapeutic efficacy, increase the cellular interaction through cationic properties, and revise the drug release profile in line with the objectives [17-19]. Therefore, various modification approaches can provide pharmaceutical advantages in the design of PCL-based nanoparticle drug delivery systems.

Recently, surface coating has aroused a great deal of interest. Surface modification materials have an essential role in fate and behavior of NPs between in biological environment. Despite the unique features of NPs, they cannot reach optimum point to show maximum impact. Surface coating of NPs with appropriate material enhances the adhesion and the retention time of NPs on target tissue [19].

Chitosan (CS) is a natural cationic polysaccharide consisting of two main units, glucosamine and N-acetylglucosamine [20]. CS has been widely preferred polymer as coating material mainly owing to its positive charge which increases the mucoadhesion of NPs. Besides, other properties of chitosan such as non-toxic, biocompatible, antimicrobial make it one of the most suitable materials for nanomedicine [21]. Poly-L-lysine (PLL) is another cationic biocompatible polymer. PLL significantly enhances cell adhesion as positively charged PLL causes interaction between NP and negatively charged cell membrane. Furthermore, PLL has good solubility in water, stable structure in biological environment as well as exerts antimicrobial effect in neutral or weak acid conditions [22].

In the present study, we prepared PCX-loaded PCL NPs as a new drug delivery system for PCX by nanoprecipitation method. In the scope of the study, passive targeting strategy was aimed for tumor targeting of nanoparticles. The passive targeting strategy is one of the most common tumor targeting approaches in nanotechnology studies. With the passive targeting approach realized due to the particle size being at the nanoscale, tumor site accumulation as a function of the size of the nanoparticles and due to the degeneration of the vasculature in the tumoral region was determined as a preliminary phenomenon [23]. NPs were coated by CS or PLL to increase cellular interaction because of their cationic charges. There are several studies that point out impact of molecular weight of PCL on characterization of NPs [23,24]. Therefore, two different kinds of PCL with different molecular weight, 14.000 and 80.000 were used in this study. In order to characterize NPs, polydispersity index, zeta potential, particle size, drug entrapment efficiency, and in vitro PCX release from PCL NPs and mathematic modeling of release kinetic were examined.

MATERIAL AND METHOD

Materials

Polycaprolactone (PCL) (Mw:14.000 and Mw:80.000)**,** Paclitaxel (Mw:853.91, ≥95% (HPLC)) and Poly-L-lysine solution (0.1% (w/v)) was purchased from Sigma–Aldrich (St. Louis, MO, USA). Chitosan (Protasan UP G-113; Mw:<200 kDa) was purchased from Novamatrix, Norway. Acetone and dialysis cellulose tubing membrane (average flat width 25 mm, MWCO: 14,000 Da) were purchased from Sigma&Aldrich, USA.

Preparation of blank and PCX-loaded PCL nanoparticles

Preparation of blank and PCX-loaded PCL NPs was carried out by nanoprecipitation method. Organic phase was prepared using two different PCL types, 14.000 and 80.000 molecular weight. For PCX-loaded PCL NPs, 10 mg PCL was weighed for each batch and 1mg of PCX was added to the organic phase. Polymer and PCX were dissolved in 5 mL acetone by magnetic stirring for 45 min. To

prepare the aqueous phase, three batches were designed according to coating material, CS and PLL. 75 mg of Pluronic F-68 and 2.5 mg chitosan or 0.01% PLL (v/v) were added to 10 mL ultra-pure water and stirred at 500 rpm at room temperature. The third group consists of NPs that do not contain any coating materials. Organic phase was added dropwise to aqueous phase at 800 rpm. In order to evaporate organic phase, solutions were mixed at 500 rpm at room temperature overnight. Dispersions were centrifuged at 3500 rpm for 5 min. Finally, in order to to remove the aggregate from solution, supernatants were filtered using 0.45 μm pore size filter. Same process was conducted for blank formulations.

Characterization of nanoparticles
Determination of particle size, PDI and zeta potential

Particle size, polydispersity index and zeta potential of PCL NPs were analysed by Malvern Zetasizer Nano ZS series, UK. All measurements were conducted at an angle of 173° for particle diameter and 12.8° for zeta potential. Measurements were performed in triplicate at room temperature. Particle size distribution was calculated as mean diameter (nm) ± standard deviation (SD) and PDI. Zeta potential (mV) was expressed as the average of three subsequent measurements ± SD.

Morphological analysis

For the determination of the surface morphology of NPs, Scanning Electron Microscopy (SEM) (Zeiss evo LS-10, Germany) was employed. The lyophilized PCL NPs were embedded on metal stubs and then coated with 100 A° thick layer of gold and palladium and dried for 24 h. The shape and surface morphology of drug loaded formulations were determined by SEM.

Determination of entrapment efficiency (EE) and drug loading (DL)

The entrapment efficiency of PCX-loaded PCL NPs was quantified directly by UV spectrophotometer. Briefly, 3 mg of the freeze-dried PCL NPs were dissolved in 300μL dichloromethane (DCM) and mixed thoroughly for 10 min so that polymer structure is disrupted and entrapped drug is released from nanoparticles. To dissolve PCX, 3 mL of methanol was added, and dichloromethane was evaporated by stirring at 500 rpm for 2 hours. Final solution was centrifuged at 3000 rpm for 5 min and supernatant was tested to determine entrapment efficiency of PCL NPs (Eq. 1 and Eq. 2). Within the scope of the validation of the spectrophotometric method for PCX quantification, linearity, specificity, precision, repeatability, limit of detection (LOD), limit of quantification (LOQ) were determined. Quantitation of PCX was determined by the validated spectrophotometric method (r^2=0.9974) at 230 nm.

DL (%) = (Weight of PCX in the NPs / Total weight of NPs) × 100   (1)

EE (%) = (Weight of PTX in NPs / Initial weight of PTX used) × 100   (2)

In vitro release of PCX from PCL nanoparticles

In vitro drug release of PCX from PCL nanoparticles were determined by using dialysis membrane (MWCO: 14,000 Da). Dialysis membrane was activated with 1% w/v NaOH overnight. PCL nanoparticle formulations loaded with PCX were prepared freshly. 2 mL of PCL NPs suspension was transferred into a dialysis membrane, hermetically sealed, and subsequently incubated in a beaker containing 75 mL phosphate buffer saline (PBS) (pH: 7.4). The system was conducted under sink conditions at 37 °C stirring at 200 rpm. At predetermined time intervals (0.5, 1, 2, 4, 8, 16, 24, 36, 48, 72, 96h), 1 mL sample was collected and replaced with fresh PBS at same volume and temperature. The amount of released PCX in PBS was analysed with UV spectrophotometer at 230 nm. Release percentage over time of the PCX-loaded PCL NPs was evaluated and plotted for each formulation.

Release kinetic studies

The release profile of PCX-loaded PCL nanoparticles was examined using DDSolver, a program intended to speed up computations and avoid computational mistakes. The resulting data were fitted to several kinetic models and examined for release mechanism (Zero order, First order, Higuchi, Korsmeyer-Peppas, Peppas-Sahlin, Weibull and Baker-Lonsdale model) [25]. After the in vitro release profiles of nanoparticles were clarified, inputs were computed using the DDSolver program to determine the four most significant and meaningful criteria: coefficient of determination (R^2), coefficient of determination adjusted ($R^2_{adjusted}$) Akaike Information Criterion (AIC), and Model Selection Criterion (MSC). The highest R^2, $R^2_{adjusted}$ and MSC values and the lowest AIC values were used to determine the best fist model [25, 26]. Additionally, using the "difference (f1)" and "similarity (f2)" factors, the release variations or similarities of PCX-loaded PCL nanoparticles were evaluated [25, 27]. In order to compare the release profiles of nanoparticles, the difference factor (f1) and similarity factor (f2) were computed using a method outlined in the Guidance for Industry from the FDA's Center for Drug Evaluation and Research (CDER) [28]. These two factors can be calculated mathematically by the following equations [29]. R and T represent the dissolved percentages of the reference and test profiles, respectively whereas t represents the time point, and n is the total number of sample points. It should be noted that f1 values for 0–15 and f2 values for 50–100 show that these release profiles are similar [30, 31].

$$f1 = \left\{ \left(\sum_{t=1}^{n} |R - T| \right) / \left(\sum_{t=1}^{n} R \right) \right\} \times 100 \tag{3}$$

$$f2 = 50 . \log \left[\frac{100}{\sqrt{1 + \frac{\sum_{t=1}^{t=n} [Rt - Tt]^2}{n}}} \right] \tag{4}$$

RESULT AND DISCUSSION

Determination of particle size, PDI and zeta potential

The particle size, PDI, and zeta potential of both types of PCL NPs are shown in Table 1. Particle size plays vital role in interaction between NPs and cell membrane, cellular uptake, penetration as well as determining the administration route. Particularly for intravenous administrations, nanoparticle diameter should be below a certain size since they might cause occlusion in blood capillaries. On the other hand, smaller particles are likely to have toxic effects due to their greater surface area [32]. Therefore, mean size of NPs should be at optimal range for *in vivo* delivery. The particle size of the developed PCL NPs ranged from 199 nm to 383 nm indicating that the size of the produced particles is in the acceptable range. The first group prepared with 80.000 MW PCL has greater particle size compared to second group prepared with 14.000 MW PCL. The main reason of this difference could be elucidated by viscosity resulted from high molecular weight. The increase of PCL molecular weight causes enhancement of viscosity in organic phase that hinders the diffusion of organic phase into aqueous phase. As a result, larger particles are formed. Our results showing that the increase of the particle size relies on molecular weight are in accordance with the data presented by Miladi et al. [23]. Particle size of uncoated NPs are between 188nm-230nm. While the particle size of CS-coated NPs ranged from 316nm-383nm, particle size of PLL-coated NPs ranged from 199nm-248nm. Both coating polymers caused an increase in particle size due to their settlement on the nanoparticle surface. This increase was higher in CS coated nanoparticles than in PLL. There are studies with similar results in the literature, and our findings were evaluated in accordance with previous studies [15, 17, 31]. As expected, surface modification had remarkable impact on particle size.

PDI values indicate homogeneity of NPs size in formulation. Values close to 0 indicate a monodisperse system while values close to 1 indicate that the system has a heterogeneous structure consisting of aggregate, polymer residues, particles with different size. As presented in Table 1, each PDI values were quite close to 0. There were also no notable variations between two types of PCL.

Zeta potential is among the most important factors affecting particle character and stability. In the literature, it is emphasized that NPs with positively charged are highly likely to interact with cell membrane since cell surface is charged negatively [23]. Yue et al. reported that positive charge encouraged the internalization of NPs to cells and further enhanced the cellular uptake. Additionally, while majority of positively charged NPs escape from lysosome, negatively or neutrally charged nanoparticles localize with lysosome [34]. According to this study, Ünal et al. stated that NPs coated with positively charged materials considerably increased the interaction between NPs and mucus layer [35]. PCL has negative surface charge because of terminal carboxylic groups. Coating materials used in the current study, PLL and CS, markedly shifted zeta potential of NPs from negative to positive. As

illustrated in Table 1, zeta potential values of uncoated NPs were all negative, between -20.1 and -25.8, while surface charge of coated NPs are range from +29.6 to +57.1. Coating materials not only altered surface charge positively but also provided higher zeta potential. Regardless of the charge type, NPs with low zeta potential tend to form aggregation owing to low electrostatic repulsive forces between the NPs [36]. In Table 1, it is clearly observed that surface modification with PLL and CS considerably rose the surface charge of NPs, from -21.4 mV to +57.1 mV. CS also showed superiority to PLL in terms of increase in zeta potential and encapsulation efficiency. It can be interpreted that CS coating has more influence on the properties of nanoparticles than PLL coating. There are studies with similar results in the literature, and our findings were evaluated in accordance with previous studies [15, 17, 31].

Table 1. Mean particle size, PDI and zeta potential of blank and PCX-loaded PCL nanoparticles prepared with different molecular weight of polymer (Organic solvent is acetone, PCL concentration is 0.2 % (w/v), CS concentration is 0.025 % (w/v), PLL concentration is 0.01 % (w/v), Pluronic F-68 concentration is 0.75% (w/v), organic phase: aqueous phase ratio 1:2 (v:v)) (n = 3, ± SD).

PCL Nanoparticle Formulations			Particle Diameter ± SD (nm)	PDI ± SD	ZP ± SD (mV)
M_w (Da)	Formulation Code	Blank/PCX loaded			
80,000	PCL NPs	Blank	209.2±1.1	0.081±0.009	-21.4±1.1
		PCX loaded	234.4±1.3	0.112±0.014	-24.9±2.1
	CS/PCL NPs	Blank	342.2±1.9	0.216±0.091	+57.1±3.1
		PCX loaded	383.8±2.4	0.253±0.122	+51.3±6.1
	PLL/PCL NPs	Blank	226.5±1.5	0.098±0.014	+34.1±3.1
		PCX loaded	248.7±1.6	0.121±0.103	+30.6±4.2
14,000	PCL NPs	Blank	188.3±1.2	0.099±0.004	-20.1±1.0
		PCX loaded	204.4±1.9	0.125±0.036	-25.8±2.3
	CS/PCL NPs	Blank	316.1±3.2	0.197±0.022	+52.3±2.3
		PCX loaded	346.2±3.9	0.224±0.018	+48.9±2.3
	PLL/PCL NPs	Blank	199.7±1.4	0.133±0.008	+31.6±1.1
		PCX loaded	227.5±1.6	0.148±0.012	+29.6±1.1
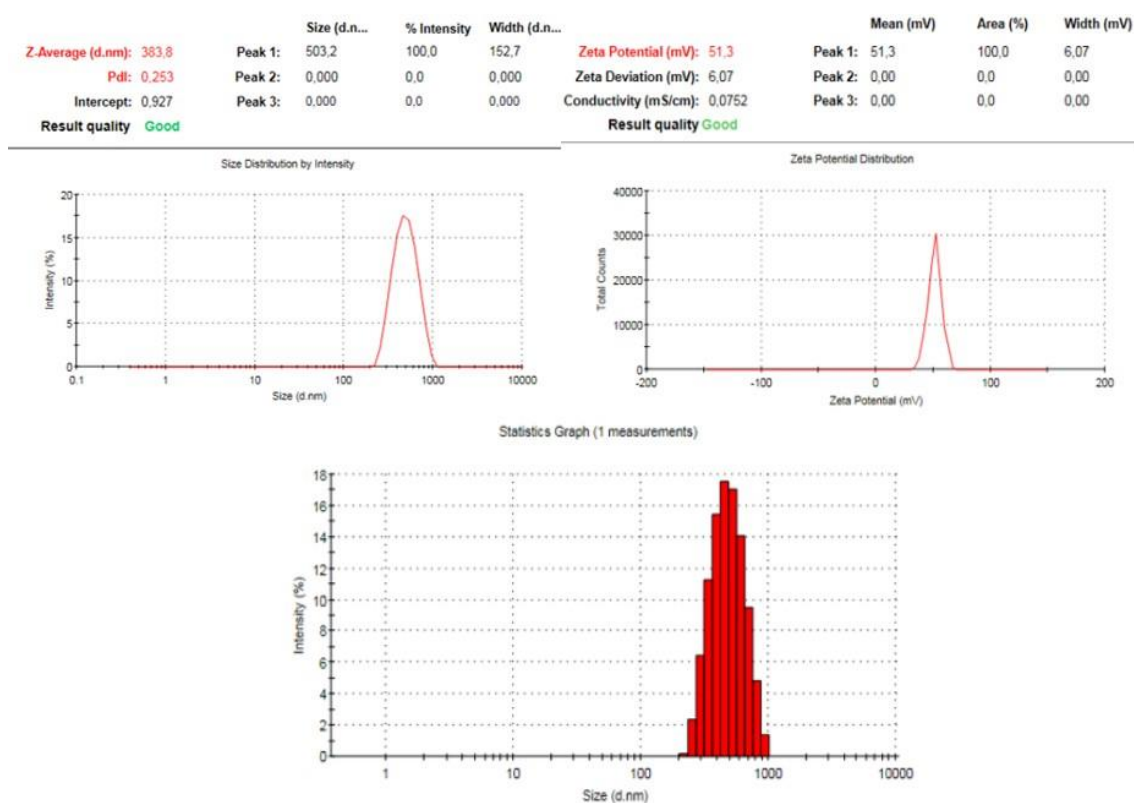
Figure 1. Analysis results of nanoparticles by Malvern zetasizer ZS. Representative images are presented for PCX-loaded CS coated PCL NPs (CS/PCX-PCL NPs) (Mw 80,000 Da) as the largest nanoparticles.

Determination of entrapment efficiency (EE) and drug loading (DL)

Table 2. summarizes the entrapment efficiency and drug loading of batches of PCX-PCL NPs prepared with two types of PCL polymer and different coating materials. Encouragingly, all prepared NPs exhibited a high entrapment rate of more than 50%. Encapsulation efficiency of NPs prepared with 80.000 MW PCL ranged from %59.4 to %64.7 while entrapment efficiency of NPs with 14.000 MW PCL varied between %51.3 and %63.1. The drug loading of PCX-loaded NPs prepared with 80.000 and 14.000 MW PCL resulted in between %6.2-8.4 and %5.2-6.6, respectively.

As it can be seen from Table 2, maximum encapsulation efficiencies were obtained with 80.000 MW of PCL. In accordance with results reported by Ali et al. and Miladi et al. NPs prepared with high molecular weight PCL showed higher encapsulation efficiency compared to NPs prepared with low molecular weight PCL [23,37]. The reason why NPs prepared with 80.000 MW PCL have higher encapsulation efficiency is the same as the reason why NPs have higher size. Increasing organic phase viscosity caused bigger particles resulting in high encapsulation efficiency. Considering the effects of coating material on encapsulation efficiency; it is clearly seen in Table 2 that minimum entrapment

ratios belonged to uncoated NPs while coating materials significantly increased encapsulation rates. This situation proves that due to the presence of coating materials, more PTX was absorbed into the surface of PCL NPs. In addition to that, NPs coated with CS had higher encapsulation efficiency than NPs coated with PLL. It can be interpreted that CS coating has more influence on the properties of nanoparticles size than PLL coating. The reason for this situation may be experimental differences, as well as the high hydrophilic character of the PLL polymer solution has a tendency to leak into the aqueous phase in the coating process. This situation was found to be compatible with similar results in previous studies [17, 31]. Also similar results regarding effect of coating material on encapsulation were presented by Badran et al. [38].

Table 2. Encapsulation efficiency (EE) and drug loading (DL) of PCX-loaded PCL nanoparticles prepared with different molecular weight of polymer.

PCL Nanoparticle Formulations		Encapsulation efficiency % ± SD (EE)	Drug loading % ± SD (DL)
M_w (Da)	Formulation Code		
80,000	PCX-PCL NPs	59.4±.1.6	6.2±0.3
	CS/PCX-PCL NPs	77.2±2.1	8.4±0.7
	PLL/PCX-PCL NPs	64.7±1.9	6.7±0.2
14,000	PCX-PCL NPs	51.3±1.1	5.2±0.1
	CS/PCX-PCL NPs	63.1±1.7	6.6±0.3
	PLL/PCX-PCL NPs	58.4±1.4	5.9±0.1

Morphological analysis

In order to elucidate the surface morphology of PCX-loaded NPs, SEM pictures were taken. Figure 2 and Figure 3 present SEM picture of NPs prepared with 14.000 MW and 80.000 MW PCL, respectively. In Figure2, size of NPs ranged between 200-310 nm, and they were in coincidence with results obtained from DLS. In Figure 3, size of NPs was 238-380 nm which shows coherence with data obtained from DLS. As seen in Figure 2 and 3, coated NPs are larger than uncoated NPs. These SEM pictures indicate that all NPs formulations have smooth and spherical surfaces.
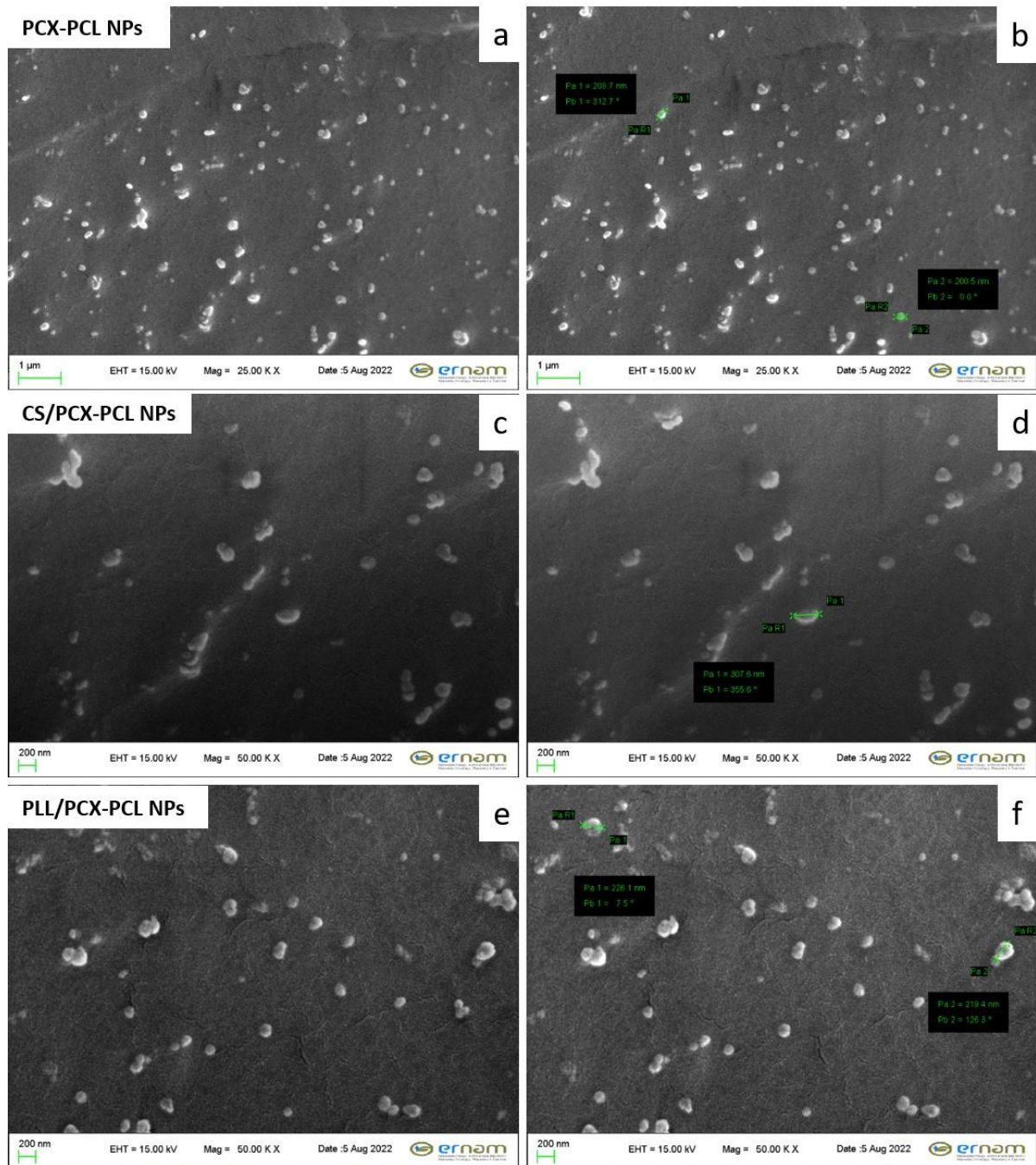
Figure 2. Scanning electron microscopy (SEM) micrographs of PCX-loaded NPs. (a, b) PCX-PCL NPs. (c, d) CS/PCX-PCL NPs. (e, f) PLL/PCX-PCL NPs. (a, b, c, d, e, f; PCL MW: 14,000Da). (b, d, f; Representative images with measuring scales)
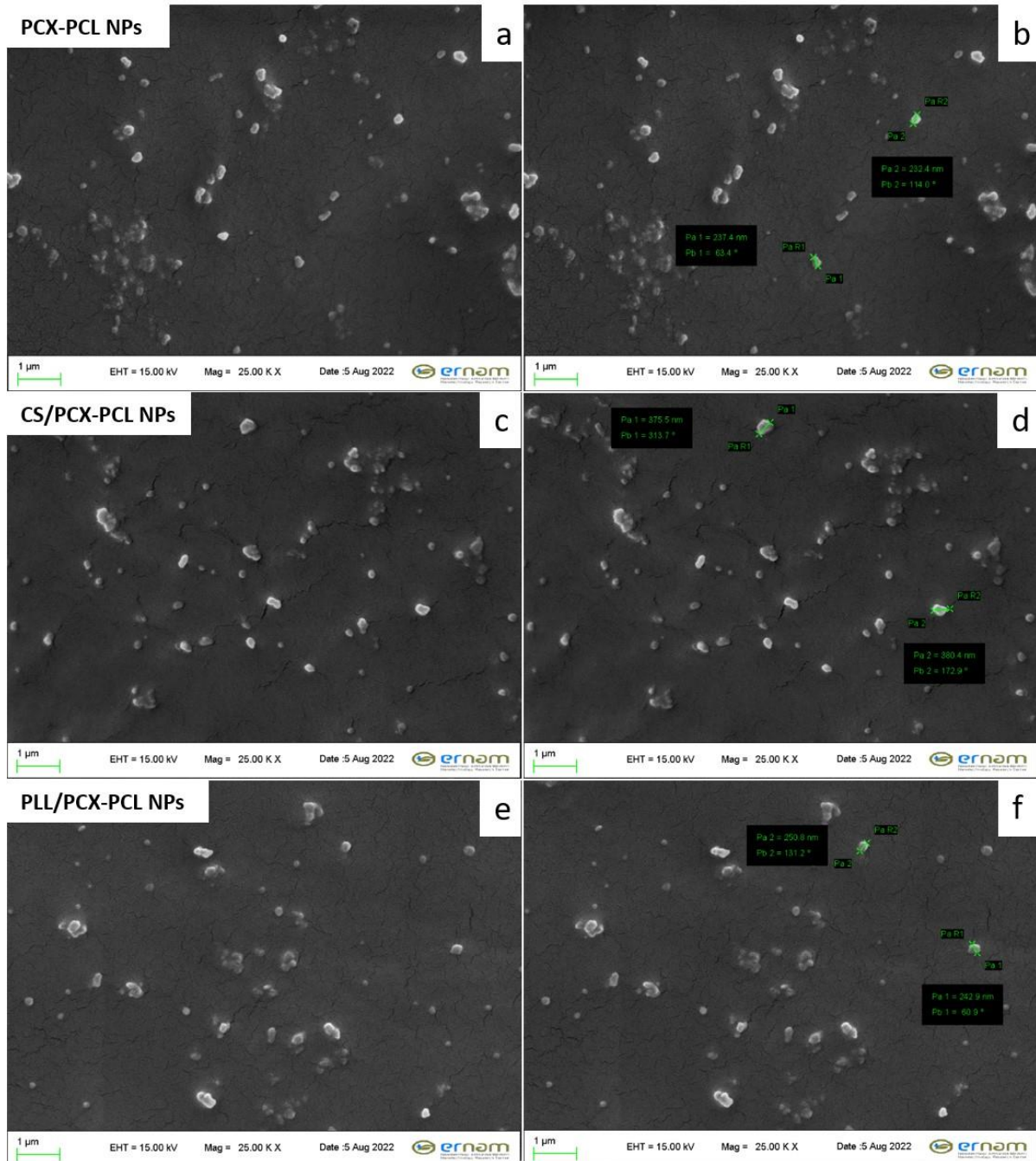
Figure 3. Scanning electron microscopy (SEM) micrographs of PCX-loaded NPs. (a, b) PCX-PCL NPs. (c, d) CS/PCX-PCL NPs. (e, f) PLL/PCX-PCL NPs. (a, b, c, d, e, f; PCL MW: 80,000Da). (b, d, f; Representative images with measuring scales).

In vitro release of PCX from PCL nanoparticles

Fig. 4 displays the *in vitro* release profiles of PCX from PCL NPs determined by using the dialysis membrane. In the light of the information obtained from the pre-formulation studies, since PCL 80.000 had higher encapsulation and drug loading, it was selected for in vitro release studies. As it can

be seen in Figure 4, PCX release from uncoated PCL formulation exhibited markedly faster profile up to 96 h in comparison with coated formulations. On the other hand, in the first 24 hour as highlighted in Figure 4, a burst release of PCX was observed for both CS and PLL coated formulations. It is believed that some of the drug which is absorbed to the coating material provides an initial fast release [39]. The reduction in the acceleration of the release profile of the coated NPs after burst effect proved this theory.

Negatively charged PCX has a stronger interaction with cationic NPS and thus, positively charged NPs extend the release time of the anionic molecules [40]. In our study, positively charged NP formulations established strong interaction with PCX and prolonged the release time of PCX from NPs. It is known that NPs with small particle size tend to exhibit faster drug release due to larger surface area [41]. As seen in Figure 4, the CS coated formulation had the slowest release profile and the uncoated PCX-PCL formulations had the faster release profile. When evaluated together with the particle sizes, according to the release profile of the formulations, smaller particles (PCX-PCL) showed a higher release rate and larger particles (CS/PCX-PCL) showed a slower release. The same is true for PLL/PCX-PCL NPs and is clearly visible. These results showed that the increase in particle size led to a decrease in the release rate, and the results were considered to be compatible with similar studies in the literature [17, 31, 41].
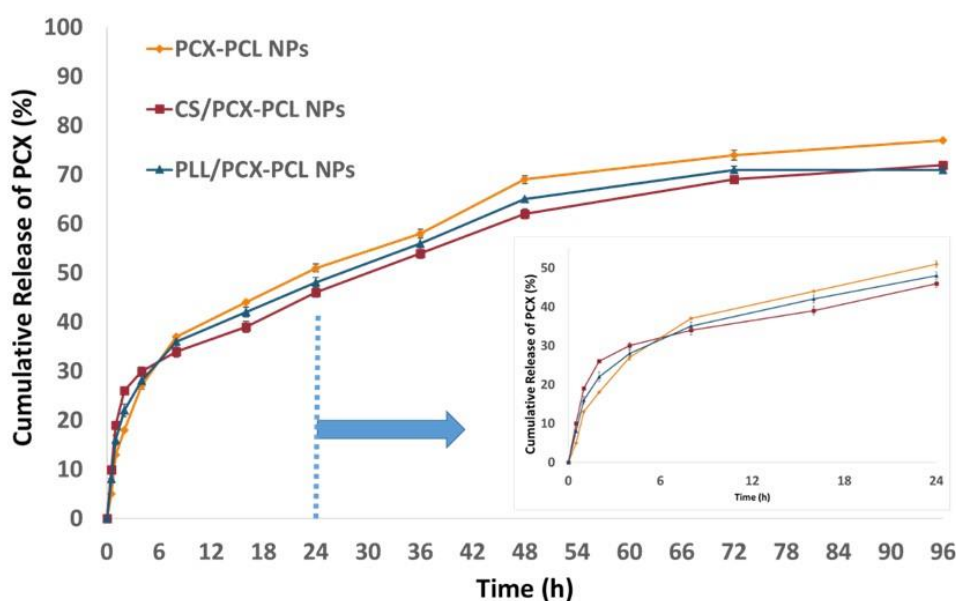
Figure 4. Release profile of PCX from PCL nanoparticles (n=3)

Release kinetic studies

In vitro dissolution test has an important role in drug development processes and quality control. It is not only a way to observe the stability of drug products but also rapid and affordable technique to

estimate fate of drug in vivo. Thus, recently quantitative examination of drug dissolution profiles has received considerable attention [25].

Kinetic modeling of PCX release from PCL NPs are demonstrated in Table 3. In order to determine the commonly used parameter (R^2, $R^2_{adjusted}$, AIC, MSC) in release kinetic, obtaining data were processed using DDSolver program. According to the results, the model having the highest R^2, $R^2_{adjusted}$, MSC as well as the lowest AIC was considered as the best-fitted one [42].

For the Weibull model, β exponent is used to explain the release from a polymeric matrix. If β is less than 0.75, it points out Fickian diffusion. 0.75< β <1 means Fickian diffusion and swelling controlled release [43]. Considering the Peppas-Sahlin model, "m" represents diffusional exponent. Release exponent ("n" for Korsemeyer-Peppas) value helps to explain how the drug released from their matrix. m≤0.45 indicates Fickian diffusion. "m" value between 0.45-0.85 indicates non-Fickian diffusion and for m=0.85 the drug release occurs through case II transport [44]. The Peppas-Sahlin and Weibull model were the two-model having highest R^2, $R^2_{adjusted}$, MSC values and lowest AIC. In other words, there was a remarkable correlation between Peppas-Sahlin and Weibull model. Our results pointed out that release of PCX from PCL NPs was predominantly driven by Fickian release. In the literature, there are studies showing consistency with our results [45, 46].

Diffusional exponent value was represented using "m" in Peppas-Sahlin and "n" in Korsmeyer-Peppas model. In the case of CS-coated NPs, Korsmeyer-Peppas model exhibited superior to portray the release of PCX. The R^2 value was 0.9858 and release exponent of Korsmeyer-Peppas (n) was 0.329. The n value lower than 0.43 indicates the approach of PCX release mechanism toward Fickian diffusion-controlled release [47]. On the other hand, data obtained from CS/PCX-PCL formulations were also well fitted by Weibull model. According to the results obtained by Weibull model, PCX release kinetics from PCL NPs was found to be compatible with Fickian diffusion. Both two models showed almost same R^2 and $R^2_{adjusted}$ values. Soares et. al. reported similar results suggesting the possibility of two models for a formulation [48].

Regarding the PLL/PCX-PCL NPs, Peppas-Sahlin and Weibull were the model with the best fitting. This means that release of PCX from PLL-coated NPs, like uncoated PCX-PCL NPs, is driven by mechanism of Fickian release [45,46].

For each formulation, similarity and difference factors were evaluated. As it can be seen in Table 4, all formulations have the difference factor below 15 and similarity factor above 50. All the formulations were similar to each other in terms of release profile. This means that although different materials were used for coating resulting in changes in properties of NPs, release profile of formulations exhibited similarity due to the use of the same polymer constructing the common structure.

Table 3. Release kinetic modeling and results of PCX-loaded PCL NPs

Model and equation / Formulation		Parameter		R^2	$R^2_{adjusted}$	AIC	MSC	n/m*
Zero-order F=k0*t	PCX-PCL	k0	1.084	0.4452	0.4452	102.8355	0.2077	-
	CS/PCX-PCL	k0	1.004	0.2343	0.2343	102.8346	-0.1918	-
	PLL/PCX-PCL	k0	1.023	0.3049	0.3049	103.0578	-0.0601	-
First-order F=100*[1-Exp(-k1*t)]	PCX-PCL	k1	0.028	0.8284	0.8284	88.7561	1.3809	-
	CS/PCX-PCL	k1	0.025	0.6319	0.6319	94.0461	0.5405	-
	PLL/PCX-PCL	k1	0.025	0.7202	0.7202	92.1401	0.8497	-
Higuchi F=kH*t^0.5	PCX-PCL	kH	9.219	0.9319	0.9319	77.6686	2.3049	-
	CS/PCX-PCL	kH	8.601	0.8650	0.8650	82.0087	1.5437	-
	PLL/PCX-PCL	kH	8.765	0.8932	0.8932	80.5806	1.8130	-
Korsmeyer-Peppas F=kKP*t^n	PCX-PCL	kKP	11.280	0.9378	0.9316	78.5728	2.2295	0.466
	CS/PCX-PCL	kKP	16.878	0.9858	0.9844	56.9837	3.6291	0.329
	PLL/PCX-PCL	kKP	14.467	0.9730	0.9703	66.0692	3.0223	0.380
Peppas-Sahlin F=k1*t^m+k2*t^(2*m)	PCX-PCL	k1	15.077	0.9918	0.9899	56.3194	4.0840	0.450
	CS/DCX-PCL	k1	15.161	0.9776	0.9726	64.4759	3.0047	0.450
	PLL/PCX-PCL	k1	15.395	0.9926	0.9909	52.6259	4.1426	0.450
Weibull F=100*{1-Exp[-((t-Ti)^β)/α]}	PCX-PCL	β	0.547	0.9930	0.9915	54.3357	4.2493	-
	CS/PCX-PCL	β	0.394	0.9830	0.9793	61.1209	3.2843	-
	PLL/PCX-PCL	β	0.449	0.9929	0.9914	51.9966	4.1950	-
Baker-Lonsdale 3/2*[1-(1-F/100)^(2/3)]-F/100=kBL*t	PCX-PCL	kBL	0.003	0.9631	0.9631	70.3079	2.9183	-
	CS/PCX-PCL	kBL	0.002	0.9193	0.9193	75.8300	2.0586	-
	PLL/PCX-PCL	kBL	0.002	0.9498	0.9498	71.5278	2.5674	-

Best fit release kinetic models for PCX-loaded PCL NPs shown with grey; In all models, F is the fraction (%) of drug released in time t, k0: zero-order release constant, k1: first-order release constant, kH: Higuchi release constant, kKP: release constant incorporating structural and geometric characteristics of the drug-dosage form, n: is the diffusional exponent indicating the drug-release mechanism, m: diffusional exponent and similar exponent like ''n'', m use in Peppas-Sahlin model equation only, α: is the scale parameter which defines the time scale of the process; β: the shape parameter which characterizes the curve as either exponential (β=1; case 1), sigmoid, S-shaped, with upward curvature followed by a turning point (β > 1; case 2), or parabolic, with a higher initial slope and after that consistent with the exponential (β < 1; case 3), Ti: the location parameter which represents the lag time before the onset of the dissolution or release process and in most cases will be near zero. Values shown in grey in the table are selections made according to criteria.

Table 4. Calculation of the differences and similarities of the release profiles of the nanoparticle formulations with the difference (f1) and similarity (f2) factors

Nanoparticle Formulation	*Difference Factor (f1)*	*Similarity Factor (f2)*
PCX-PCL NPs and CS/PCX-PCL	*11.84*	*64.35*
PCX-PCL NPs and PLL/PCX-PCL	*6.98*	*74.21*
PLL/PCX-PCL NPs and CS/PCX-PCL	5.42	79.82
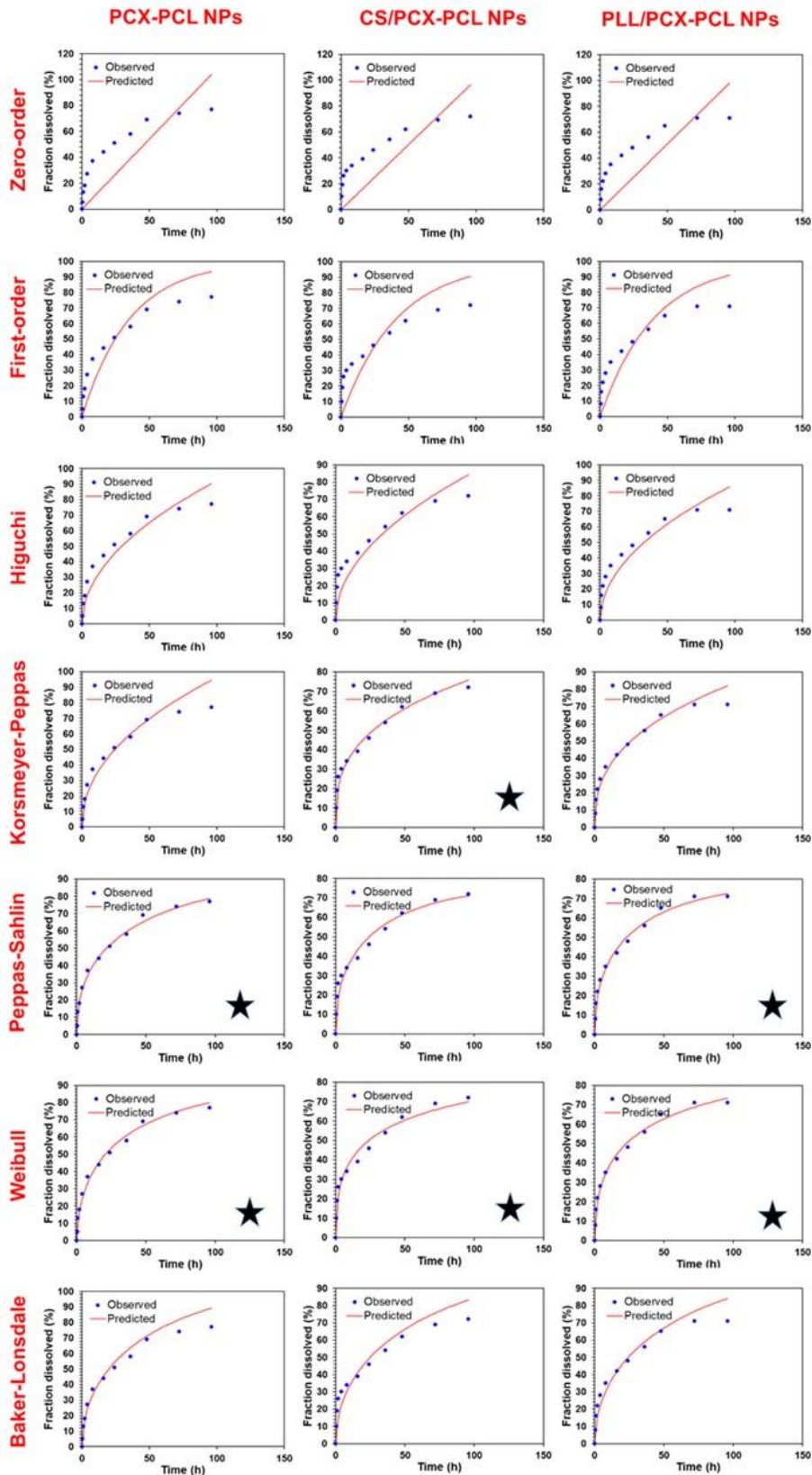
Figure 5. Mathematical model fitting of PCX release from PCL NPs for Zero-order, first-order, Higuchi, Korsmeyer-Peppas, Peppas-Sahlin, Weibull and Baker-Lonsdale models (*best fit models).

In this study, our aim was to prepare PCX-loaded PCL NPs by the nanoprecipitation method and to elucidate the *in vitro* characteristics and release kinetic mechanisms of PCL NPs. Six formulations were prepared with using PCL with two different molecular weight and different coating material in order to observe influence of both molecular weight and coating material on characterization of NPs. According to the results, high molecular weight PCL increased the particle size but increased the encapsulation efficiency. With the cationic coating, the zeta potential of the nanoparticles could be made positively charged. On the other hand, coating materials significantly increased the particle size and encapsulation efficiency, as well. Coating materials also provided longer release time compared to uncoated formulation. Considering the mathematical modeling of release kinetic, the release profile of PCX-PCL NPs and PLL/PCX-PCL were compatible with Peppas-Sahlin and Weibull model. Korsmeyer-Peppas and Weibull model was superior to describe the release of PCX from CS-coated PCL NPs. For each formulation, PCX release kinetic from PCL NPs was compatible Fickian diffusion. This study constitutes a preliminary research for the PCX-loaded PCL NPs to increase the therapeutic efficacy in lung cancer.

AUTHOR CONTRIBUTIONS

Concept: *S.Ü., O.D.*; Design: *S.Ü, O.D.*; Control: S.*Ü., O.D., Y.A.*; Sources: *S.Ü., O.D., Y.A.*; Materials: *S.Ü., O.D., Y.A.*; Data Collection and/or processing: *S.Ü., O.D., Y.A.*; Analysis and/or interpretation: *S.Ü., O.D., Y.A.*; Literature review: *S.Ü., O.D., Y.A.*; Manuscript writing: S.*Ü., O.D., Y.A.*; Critical review: *S.Ü., O.D., Y.A.*; Other: *S.Ü.*

CONFLICT OF INTEREST

The authors declare that there is no real, potential, or perceived conflict of interest for this article.

ETHICS COMMITTEE APPROVAL

The authors declare that the ethics committee approval is not required for this study.

REFERENCES

1. Sung, H., Ferlay, J., Siegel, R. L., Laversanne, M., Soerjomataram, I., Jemal, A., Bray, F. (2021). Global cancer statistics 2020: GLOBOCAN estimates of incidence and mortality worldwide for 36 cancers in 185 countries. *CA: A Cancer Journal for Clinicians*, *71*(3), 209-249. [CrossRef]

2.   Houston, K. A., Henley, S. J., Li, J., White, M. C., Richards, T. B. (2014). Patterns in lung cancer incidence rates and trends by histologic type in the United States, 2004-2009. *Lung Cancer*, *86*(1), 22-28. [CrossRef]

3.   Zarogoulidis, K., Zarogoulidis, P., Darwiche, K., Boutsikou, E., Machairiotis, N., Tsakiridis, K., Katsikogiannis, N., Kougioumtzi, I., Karapantzos, I., Huang, H., Spyratos, D. (2013). Treatment of non-small cell lung cancer (NSCLC). *Journal of Thoracic Disease*, *5* (Suppl 4), S389-S396. [CrossRef]

4.   Zappa, C., Mousa, S. A. (2016). Non-small cell lung cancer: Current treatment and future advances. *Translational Lung Cancer Research*, *5*(3), 288-300. [CrossRef]

5.   Mangal, S., Gao, W., Li, T., Zhou, Q. T. (2017). Pulmonary delivery of nanoparticle chemotherapy for the treatment of lung cancers: Challenges and opportunities. *Acta Pharmacologica Sinica*, *38*(6), 782-797. [CrossRef]

6.   Chandolu, V., Dass, C. R. (2013). Treatment of lung cancer using nanoparticle drug delivery systems. *Current Drug Discovery Technologies*, *10*(2), 170-176. [CrossRef]

7.   Massey, A. E., Sikander, M., Chauhan, N., Kumari, S., Setua, S., Shetty, A. B., Mandil, H., Kashyap, V. K., Khan, S., Jaggi, M., Yallapu, M. M., Hafeez, B. B., Chauhan, S. C. (2019). Next-generation paclitaxel-nanoparticle formulation for pancreatic cancer treatment. *Nanomedicine: Nanotechnology, Biology, and Medicine*, *20*, 102027. [CrossRef]

8.   Xiao, H., Verdier-Pinard, P., Fernandez-Fuentes, N., Burd, B., Angeletti, R., Fiser, A., Horwitz, S. B., Orr, G. A. (2006). Insights into the mechanism of microtubule stabilization by Taxol. *Proceedings of the National Academy of Sciences of the United States of America*, *103*(27), 10166-10173. [CrossRef]

9.   Shurin, G. V., Tourkova, I. L., Shurin, M. R. (2008). Low-dose chemotherapeutic agents regulate small Rho GTPase activity in dendritic cells. *Journal of Immunotherapy*, *31*(5),491-499. [CrossRef]

10.   Ruttala, H. B., Ko, Y. T. (2015). Liposome encapsulated albumin-paclitaxel nanoparticle for enhanced antitumor efficacy. *Pharmaceutical Research*, *32*(3), 1002-1016. [CrossRef]

11.   Bernabeu, E., Helguera, G., Legaspi, M. J., Gonzalez, L., Hocht, C., Taira, C., Chiappetta, D. A. (2014). Paclitaxel-loaded PCL-TPGS nanoparticles: In vitro and in vivo performance compared with Abraxane®. *Colloids and Surfaces. B, Biointerfaces*, *113*, 43-50. [CrossRef]

12.   Lukyanov, A. N., Torchilin, V. P. (2004). Micelles from lipid derivatives of water-soluble polymers as delivery systems for poorly soluble drugs. *Advanced Drug Delivery Reviews*, *56*(9), 1273-1289.[CrossRef]

13.   Joshi, K., Chandra, A., Jain, K., Talegaonkar, S. (2019). Nanocrystalization: An emerging technology to enhance the bioavailability of poorly soluble drugs. *Pharmaceutical Nanotechnology*, *7*(4), 259-278. [CrossRef]

14.   Thamake, S. I., Raut, S. L., Ranjan, A. P., Gryczynski, Z., Vishwanatha, J. K. (2011). Surface functionalization of PLGA nanoparticles by non-covalent insertion of a homo-bifunctional spacer for active targeting in cancer therapy. *Nanotechnology*, *22*(3), 035101. [CrossRef]

15. Bilensoy, E., Sarisozen, C., Esendağli, G., Doğan, A. L., Aktaş, Y., Sen, M., Mungan, N. A. (2009). Intravesical cationic nanoparticles of chitosan and polycaprolactone for the delivery of Mitomycin C to bladder tumors. *International Journal of Pharmaceutics*, *371*(1-2), 170-176. [CrossRef]

16. W. Badri W., El Asbahani, A., Miladi, K., Baraket, A., Agusti, G., Nazari, Q. A., Errachid,A., Fessi, H., Elaissari, A. (2018). Poly (ε-caprolactone) nanoparticles loaded with indomethacin and Nigella Sativa L. essential oil for the topical treatment of inflammation. *Journal of Drug Delivery Science and Technology*, *46*, 234-242. [CrossRef]

17. Varan, C., Bilensoy, E. (2017). Cationic PEGylated polycaprolactone nanoparticles carrying post-operation docetaxel for glioma treatment. *Beilstein Journal of Nanotechnology*, *8*, 1446-1456. [CrossRef]

18. Jia, W., Gu, Y., Gou, M., Dai, M., Li, X., Kan, B., Yang, J., Song, Q., Wei, Y., Qian, Z. (2008). Preparation of biodegradable polycaprolactone/poly (ethylene glycol)/polycaprolactone (PCEC) nanoparticles. *Drug Delivery*, *15*(7), 409-416. [CrossRef]

19. Lima, I. A., Khalil, N. M., Tominaga, T. T., Lechanteur, A., Sarmento, B., Mainardes, R. M. (2018). Mucoadhesive chitosan-coated PLGA nanoparticles for oral delivery of ferulic acid. *Artificial Cells, Nanomedicine, and Biotechnology*, *46*(sup2), 993-1002. [CrossRef]

20. Cheung, R. C., Ng, T. B., Wong, J. H., Chan, W. Y. (2015). Chitosan: An update on potential biomedical and pharmaceutical applications. *Marine Drugs*, *13*(8), 5156-5186. [CrossRef]

21. Prabaharan, M. (2008). Review paper: Chitosan derivatives as promising materials for controlled drug delivery. *Journal of Biomaterials Applications*, *23*(1), 5-36. [CrossRef]

22. Yuan, Y., Shi, X., Gan, Z., Wang, F. (2018). Modification of porous PLGA microspheres by poly-l-lysine for use as tissue engineering scaffolds. *Colloids and Surfaces. B, Biointerfaces*, *161*, 162-168. [CrossRef]

23. Miladi, K., Sfar, S., Fessi, H., Elaissari, A. (2015). Encapsulation of alendronate sodium by nanoprecipitation and double emulsion: From preparation to in vitro studies. *Industrial Crops and Products*, *72*, 24-33. [CrossRef]

24. Jesus, S., Bernardi, N., da Silva, J., Colaço, M., Panão Costa, J., Fonte, P., Borges, O. (2020). Unravelling the immunotoxicity of polycaprolactone nanoparticles-effects of polymer molecular weight, hydrolysis, and blends. *Chemical Research in Toxicology*, *33*(11), 2819-2833. [CrossRef]

25. Zhang, Y., Huo, M., Zhou, J., Zou, A., Li, W., Yao, C., Xie, S. (2010). DDSolver: An add-in program for modeling and comparison of drug dissolution profiles. *The AAPS Journal*, *12*(3), 263-271. [CrossRef]

26. Gamal, A., Saeed, H., El-Ela, F., Salem, H. F. (2021). Improving the antitumor activity and bioavailability of sonidegib for the treatment of skin cancer. *Pharmaceutics*, *13*(10), 1560. [CrossRef]

27. Murtaza, G., Ahmad, M., Khan, S. A., Hussain, I. (2012). Evaluation of cefixime-loaded chitosan microspheres: Analysis of dissolution data using DDSolver. *Dissolution Technologies, 19*(2), 13-19. [CrossRef]

28. FDA, U. (1997). Guidance for Industry: Dissolution testing of immediate-release solid oral dosage forms. *Food and Drug Administration, Center for Drug Evaluation and Research (CDER)*, 1-11.

29. Aldeek, F., McCutcheon, N., Smith, C., Miller, J. H., Danielson, T. L. (2021). Dissolution testing of nicotine release from OTDN pouches: Product characterization and product-to-product comparison. *Separations*, *8*(1), 7. [CrossRef]

30. Puthli, S., Vavia, P. R. (2009). Stability studies of microparticulate system with piroxicam as model drug. *AAPS Pharmscitech*, *10*(3), 872-880. [CrossRef]

31. Moore, T., Shangraw, R., Habib, Y. (1996). In dissolution calibrator tablets: A recommendation for new calibrator tablets to replace both current USP calibrator tablets. *Pharmacopeial Forum*, pp:2423-2428.

32. Yang, W., Wang, L., Mettenbrink, E. M., DeAngelis, P. L., Wilhelm, S. (2021). Nanoparticle Toxicology. *Annual Review of Pharmacology and Toxicology*, *61*(1), 269-289. [CrossRef]

33. Mailänder, V., Landfester, K. (2009). Interaction of nanoparticles with cells. *Biomacromolecules*, *10*(9), 2379–2400. [CrossRef]

34. Yue, Z. G., Wei, W., Lv, P. P., Yue, H., Wang, L. Y., Su, Z. G., Ma, G. H. (2011). Surface charge affects cellular uptake and intracellular trafficking of chitosan-based nanoparticles. *Biomacromolecules*, *12*(7), 2440–2446. [CrossRef]

35. Ünal, H., d'Angelo, I., Pagano, E., Borrelli F., Izoo A., Ungaro F., Quaglia F., Bilensoy E. (2015). Core–shell hybrid nanocapsules for oral delivery of camptothecin: Formulation development, in vitro and in vivo evaluation. *Journal of Nanoparticle Research, 17***,** 42. [CrossRef]

36. Chigumira, W., Maposa, P., Gadaga, L.L., Dube, A., Tagwireyi, D., Maponga, C. C. (2015). Preparation and evaluation of pralidoxime-loaded PLGA nanoparticles as potential carriers of the drug across the blood brain barrier. *Journal of Nanomaterials*, *2015*, 1-5. [CrossRef]

37. Ali, R., Farah, A., Binkhathlan, Z. (2017). Development and characterization of methoxy poly(ethylene oxide)-*block*-poly(ε-caprolactone) (PEO-*b*-PCL) micelles as vehicles for the solubilization and delivery of tacrolimus. *Saudi Pharmaceutical Journal : SPJ : The Official Publication of the Saudi Pharmaceutical Society*, *25*(2), 258-265. [CrossRef]

38. Badran, M. M., Alomrani, A. H., Harisa, G. I., Ashour, A. E., Kumar, A., Yassin, A. E. (2018). Novel docetaxel chitosan-coated PLGA/PCL nanoparticles with magnified cytotoxicity and bioavailability. *Biomedicine & Pharmacotherapy = Biomedecine & Pharmacotherapie*, *106*, 1461-1468. [CrossRef]

39. Ubrich, N., Bouillot, P., Pellerin, C., Hoffman, M., Maincent, P. (2004). Preparation and characterization of propranolol hydrochloride nanoparticles: A comparative study. *Journal of Controlled Release: Official Journal of the Controlled Release Society*, *97*(2), 291-300. [CrossRef]

40. Varan, G., Benito, J. M., Mellet, C. O., Bilensoy, E. (2017). Development of polycationic amphiphilic cyclodextrin nanoparticles for anticancer drug delivery. *Beilstein Journal of Nanotechnology*, *8*, 1457-1468. [CrossRef]

41. Mora-Huertas, C. E., Fessi, H., Elaissari, A. (2010). Polymer-based nanocapsules for drug delivery. *International Journal of Pharmaceutics*, *385*(1-2), 113-142. [CrossRef]

42. Azadi, A., Hamidi, M., Rouini, M. R. (2013). Methotrexate-loaded chitosan nanogels as 'Trojan Horses' for drug delivery to brain: Preparation and in vitro/in vivo characterization. *International Journal of Biological Macromolecules*, *62*, 523-530. [CrossRef]

43. Papadopoulou, V., Kosmidis, K., Vlachou, M., Macheras, P. (2006). On the use of the Weibull function for the discernment of drug release mechanisms. *International Journal of Pharmaceutics*, *309*(1-2), 44-50. [CrossRef]

44. Unagolla, J. M., Jayasuriya, A. C. (2018). Drug transport mechanisms and in vitro release kinetics of vancomycin encapsulated chitosan-alginate polyelectrolyte microparticles as a controlled drug delivery system. *European Journal of Pharmaceutical Sciences: Official Journal of the European Federation for Pharmaceutical Sciences*, *114*, 199-209. [CrossRef]

45. Öztürk, A. A., Yenilmez, E., Özarda, M. G. (2019). Clarithromycin-loaded poly (lactic-*co*-glycolic acid) (PLGA) nanoparticles for oral administration: Effect of polymer molecular weight and surface modification with chitosan on formulation, nanoparticle characterization and antibacterial effects. *Polymers*, *11*(10), 1632. [CrossRef]

46. Yang, H., Li, J., Patel, S. K., Palmer, K. E., Devlin, B., Rohan, L. C. (2019). Design of poly(lactic-*co*-glycolic Acid) (PLGA) nanoparticles for vaginal co-delivery of griffithsin and dapivirine and their synergistic effect for HIV prophylaxis. *Pharmaceutics*, *11*(4), 184. [CrossRef]

47. Supramaniam, J., Adnan, R., Mohd Kaus, N. H., Bushra, R. (2018). Magnetic nanocellulose alginate hydrogel beads as potential drug delivery system. *International Journal of Biological Macromolecules*, *118*(PtA), 640-648. [CrossRef]

48. Soares, P., Sousa, A. I., Silva, J. C., Ferreira, I., Novo, C., Borges, J. P. (2016). Chitosan-based nanoparticles as drug delivery systems for doxorubicin: Optimization and modelling. *Carbohydrate Polymers*, *147*, 304-312. [CrossRef]